



Universidade de São Paulo

Biblioteca Digital da Produção Intelectual - BDPI

Departamento de Física e Ciências Materiais - IFSC/FCM

Artigos e Materiais de Revistas Científicas - IFSC/FCM

2014-05

Femtosecond laser fabrication of waveguides in DR13-doped PMMA

Optics Communications, Amsterdam : Elsevier BV, v. 318, p. 53-56, May 2014
<http://www.producao.usp.br/handle/BDPI/50802>

Downloaded from: Biblioteca Digital da Produção Intelectual - BDPI, Universidade de São Paulo



Femtosecond laser fabrication of waveguides in DR13-doped PMMA



P.H.D. Ferreira*, R. Stefanutti, F.J. Pavinatto, C.R. Mendonça

Instituto de Física de São Carlos, Universidade de São Paulo, Caixa Postal 369, 13560-970 São Carlos, SP, Brazil

ARTICLE INFO

Article history:

Received 9 September 2013

Received in revised form

17 December 2013

Accepted 21 December 2013

Available online 7 January 2014

Keywords:

Microfabrication

Waveguides

Femtosecond lasers

Polymers

ABSTRACT

This work demonstrated the fabrication of tubular waveguides in bulk samples of PMMA doped with Disperse Red 13 (DR13) by oscillator only fs-laser micromachining. We studied the influence of the incident pulse energy on the diameter and quality of the fabricated waveguides by analyzing optical microscopy images. HeNe laser (632.8 nm) was coupled into the fabricated waveguides, revealing an annular intensity distribution resulting from the superposition of propagation modes with azimuthal symmetry. The averaged total loss of the fabricated waveguides was estimated as 0.8 dB/mm. Residual birefringence was observed in the produced waveguides, probably generated during the fabrication process, which prevented determining optically induced birefringence owing to the presence of the azochromophore DR13.

© 2014 Published by Elsevier B.V.

1. Introduction

In the last decade years, femtosecond lasers have been largely used for the production of microstructures such as interferometers, waveguide couplers and decouplers, gratings, switches, and amplifiers [1–8]. The use of fs-laser micromachining has some advantages in relation to other techniques employed for waveguide fabrication, such as photolithography, high-energy ion implantation and reactive ion etching [9]. The latter methods often need prior design and fabrication of masks, being inherently planar technologies that require numerous processing steps. On the contrary, fs-laser fabrication allows single-step, maskless and direct processing [9–12]. Furthermore, micromachining with fs-laser pulses allows the production of 3D micro- and nano-structures [13].

The interest on developing polymer-based optical technologies has grown in the last years because they present some advantages over glass, such as easiness of processing and fabrication and low cost of production. Moreover, polymeric materials can be engineered to present certain properties such as, for instance, electro-optic coefficient, nonlinear optical response and enhanced photosensitivity aiming at applications [14], such as optical storage and electro-optic modulators. In particular, poly(methyl methacrylate) (PMMA), whose monomer molecular structure is shown in Fig. 1(a), is an inexpensive and widely used polymer for the production of optical components due to its high transmission in the visible and near-infrared, and the similarity of its refractive index to that of standard optical fibers, which favors coupling to existing fiber technologies. For example, the first demonstration of tubular

waveguides in PMMA was reported by Zoubir et al. [15]. Furthermore, organic chromophores or inorganic compounds, such as rare-earth ions [16], can be incorporated into its polymeric matrix to develop devices aiming at specific applications [17].

In this paper we demonstrate the fabrication of waveguides by femtosecond laser micromachining in PMMA doped with the chromophore Disperse Red 13 (DR13) [18,19]. DR13 is an azoaromatic chromophore, also known as azochromophore, whose molecular structure is presented in Fig. 1(b). Azochromophores possesses interesting linear and nonlinear optical properties, which can be exploited for electro-optic modulators [20], second-harmonic generation [21] and birefringent devices [22,23]. After studying the experimental conditions for waveguides fabrication in the PMMA/DR13, which presented tubular structure, they were characterized by optical microscopy. We demonstrated the functionality of the fabricated waveguides by measuring the near-field intensity distribution at the waveguide output, as well as its guiding efficiency. Because the produced waveguides presented residual birefringence, generated during fs-laser fabrication, we have not been able to observe any optically induced birefringence, although it was observed in bulk PMMA/DR13.

2. Experimental

The PMMA/DR13 sample was prepared by bulk polymerization. [4'[[2-(methacryloyloxy) ethyl] ethylamino]-2-chloro-4-nitroazobenzene methacrylate] DR13Ma (Aldrich) was used as obtained. Methyl methacrylate (MMA) (Aldrich) was distilled before use. The bulk polymerization was carried out in a glass ampoule in which 18.72 g (0.1872 mol) of MMA, 0.021 g (5.037×10^{-6} mol) of DR13Ma and 0.0032 g of 2,2-azobisisobutyronitrile (AIBN) were added. The ampoule was cooled in liquid nitrogen and placed in a vacuum before

* Corresponding author. Tel.: +55 16 3373 8085x211.

E-mail addresses: paulohdf@gmail.com,
paulohdf@ursa.ifsc.usp.br (P.H.D. Ferreira).

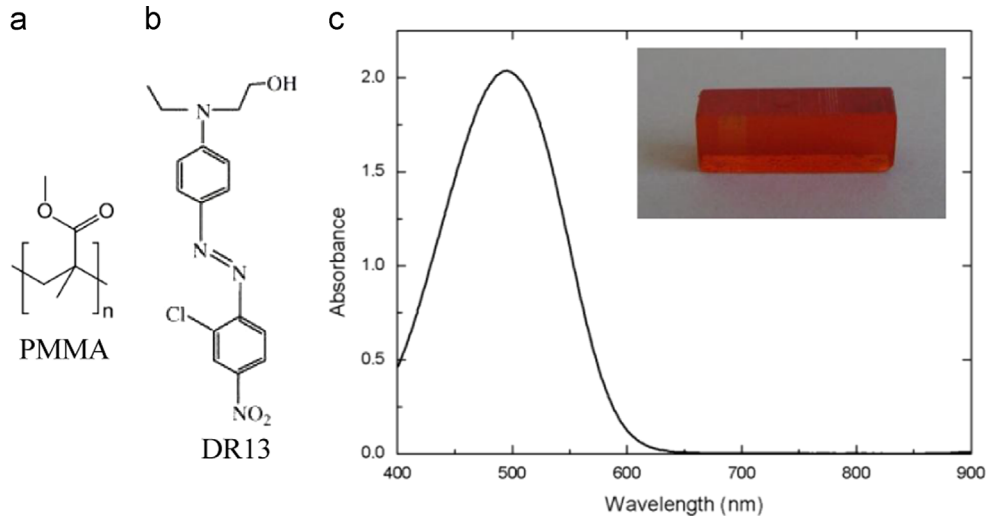


Fig. 1. Molecular structures of the PMMA (a) and DR13 (b). DR13-doped PMMA absorption spectrum (c). The inset shows a picture of the sample.

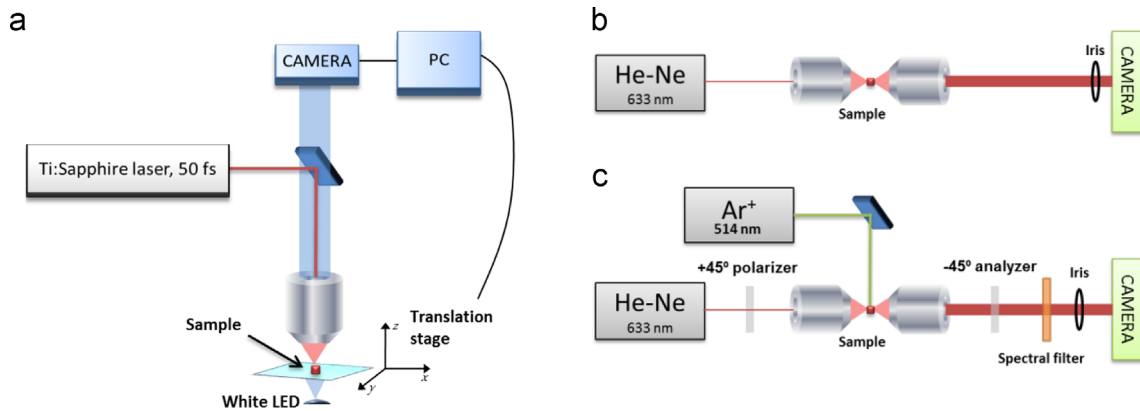


Fig. 2. Micromachining (a), waveguide coupling (b) and birefringence measurement (c) systems.

sealing. Subsequently it was allowed to attain room temperature and then heated to 60 °C in an oven for 2 h. The ampoule was broken and the solid material was cut in pieces of $10 \times 5 \times 3 \text{ mm}^3$ and polished using a wax base for polishing.

The absorbance spectrum of the bulk PMMA/DR13 sample, displayed in the inset of Fig. 1(c), was obtained with a spectrophotometer. As can be seen in Fig. 1(c), there is no absorption around 800 nm, wavelength used for the waveguide fabrication with fs-pulses. At 632.8 nm, wavelength in which the produced waveguides were tested, the absorbance of the sample was measured as 0.016.

For the waveguides fabrication, the samples were micromachined using an extended-cavity Ti:Sapphire laser oscillator, with a repetition rate of 5.2 MHz and a $\sim 25\text{-nm}$ (FWHM) spectral bandwidth centered at 800 nm, that produces 100 nJ energy pulses with 50 fs of duration. The pulses were tightly focused through a $40 \times$ (0.67-NA) microscope objective into the sample, which was translated at a constant speed of $100 \mu\text{m/s}$ with respect to the laser beam. The schematic setup can be seen in Fig. 2(a). Waveguides were written along the entire 3-mm length of the sample, and spaced by $100 \mu\text{m}$ to prevent crosstalk between them. After micromachining, the ends of the sample were polished to allow coupling of light into the waveguides. The final length of the waveguides was 2.3 mm. Fig. 2(b) shows an illustration of the experimental setup for coupling light in the waveguide. Before reaching the first microscope lens ($20 \times -9 \text{ mm}$ of effective focal length), the HeNe (632.8 nm) laser beam was spatially filtered and expanded by a telescope. An iris, placed right before the objective,

is used to control the beam diameter and thus the numerical aperture (NA) of the beam incident on the waveguide. The light transmitted through the waveguide is collected by a $20 \times$ microscope objective at the exit. Besides, an iris was used to block any scattered light at the exit of the second objective lens. The exit of the waveguide was imaged on a CCD camera to analyze the guided mode. In order to determine the total loss (coupling+propagation) of the fabricated waveguides, we measured the laser beam power before and after the coupling system (Fig. 2(b)), taking into account all transmission factors of the system. The setup for measuring the optically induced birefringence of the sample, displayed in Fig. 2(c), a polarizer ($+45^\circ$) and an analyzer (-45°) are placed, respectively, before the entrance objective and after the exit objective. A polarized cw Ar^+ laser (writing beam), operating at 514 nm, was used as the excitation source to induce the orientation of the azochromophores, which leads to the optically induced birefringence. The sample was irradiated with the Ar^+ laser for 60 s, which guarantees that molecular orientation reached saturation. A color filter is placed in front of the camera to block any light scattered from the writing laser.

3. Results and discussion

For the waveguides fabrication, the fs-laser beam is focused into a 3-mm-thick PMMA/DR13 sample, approximately $120 \mu\text{m}$ below the surface, with different pulse energies, producing

waveguides with different diameters. Fig. 3 shows the dependence of the diameter of the waveguides as a function of pulse energy. We produced five groups (corresponding to five distinct energies) with four waveguides, each one separated by $100\ \mu\text{m}$ to avoid crosstalk. As seen in Fig. 3, there is a growth of the waveguides

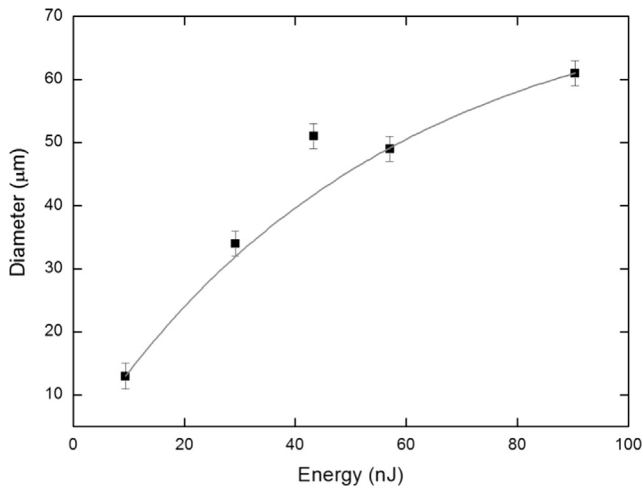


Fig. 3. Diameter of the produced waveguides as a function of the incident pulse energy and constant sample velocity ($100\ \mu\text{m/s}$).

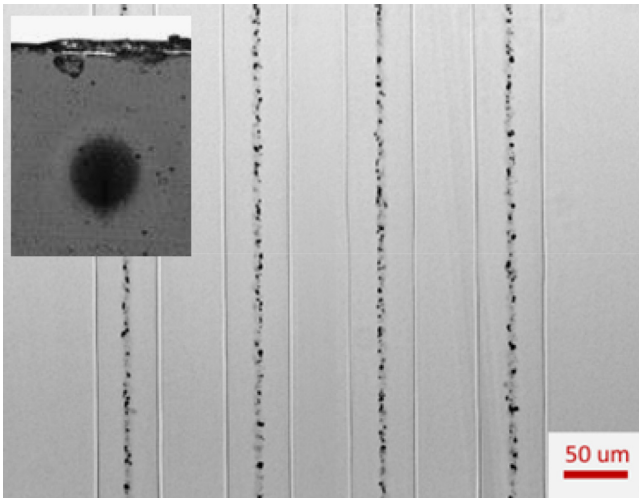


Fig. 4. Optical microscopy image of waveguides produced with an energy of $42\ \text{nJ}$ and scanning speed of $100\ \mu\text{m/s}$. The inset shows a transverse image of a typical waveguide.

diameter with the pulse energy, from approximately 10 to $60\ \mu\text{m}$ when the energy varies from 10 to $90\ \text{nJ}$. The diameters were calculated by the average value of each group. The solid line in Fig. 3 was drawn only to guide the eye.

After the waveguides fabrication, they were characterized by optical microscopy. Fig. 4 shows the top view of the third group of waveguides, fabricated with $42\ \text{nJ}$. As it can be seen, randomly black dots were formed in the center of the waveguides (in a region of about $5\ \mu\text{m}$), for all energy used, probably due to thermal degradation at the zone surrounding the laser focus spot, where the material experience high enough intensities that leads to carbonization [18]. Such black dots pattern has also been reported when fs-laser is used to fabricate waveguides in PMMA [24], using approximately the same conditions reported here. The inset in Fig. 4 shows a transverse image (cross-sectional view) of one of the produced waveguides.

Fig. 5(a) shows a transmission optical microscopy image of the fs-laser micromachined waveguide in PMMA/DR13. Generally, upon femtosecond laser irradiation, a positive refractive index change is observed in many materials, such as fused silica [25,26] and chalcogenide glass [27]. It has also been reported that when PMMA is exposed to fs-laser pulses, a negative refractive index change is produced at the center of the exposed region [15], that is characterized by a darker region. Others authors also report negative index change over a wide repetition rate range ($100\ \text{kHz}$ to $1\ \text{MHz}$) [28]. From Fig. 5(a), we have also observed that the center of the fabricated waveguide appears darker (region A). However, considering the black dots that were formed during the fabrication (Fig. 4), we believe that the darker region in Fig. 5(a) may also be due to absorption of such structures. Another possible reason for the depressed refractive index is thermal unzipping degradation [28] and even scattering of the light by the black dots. In the lighter region, surrounding the focus spot (B), a positive index change is observed, resulting in an annular refractive index distribution. This feature is caused by the thermal expansion in the focus followed by rapid cooling, that depends upon exact microfabrication conditions, leading to an increased optical density in the surrounding region by thermally induced stress. Similar behavior has been observed in other materials, such as phosphate glass [26] and crystalline materials [29,30].

After initial alignment, light from HeNe laser beam can easily be coupled into the waveguides. We show in Fig. 5(b) the near-field intensity distribution at the output of the waveguide. Although there is no guiding in the center due to absorption, light was guided in an annular region (higher index refraction) by total internal reflection. There can also be seen that there is several modes with azimuthal symmetry, whose number is proportional to the waveguide diameter.

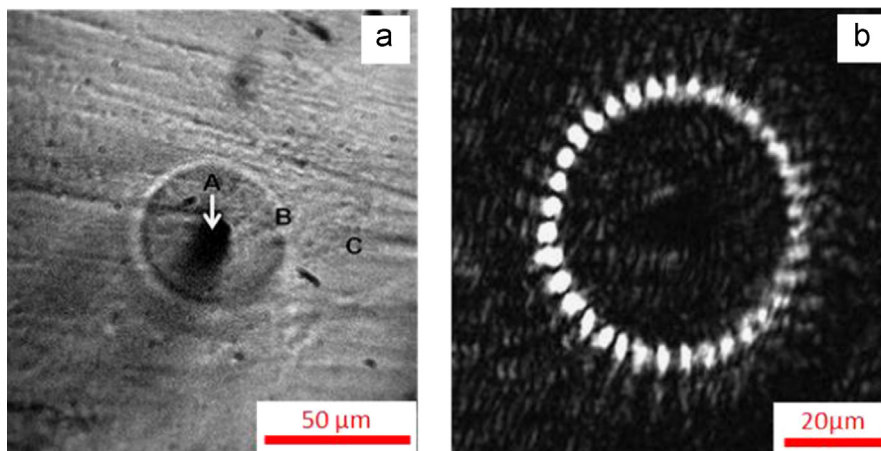


Fig. 5. Transmissive optical microscopy (a) and near-field intensity distribution of the output of the waveguide (b).

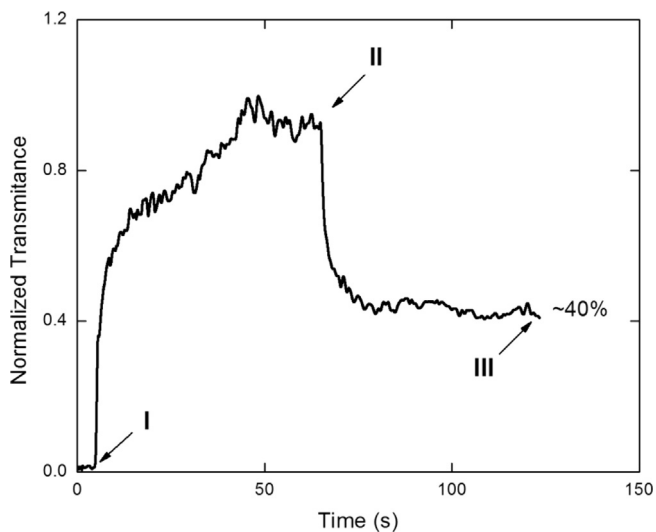


Fig. 6. Optically induced birefringence curve of PMMA/DR13 bulk sample.

To estimate the total loss, we measured the laser beam power before and after the coupling system, taking into account all transmission factors. The produced waveguides present a total loss of 0.8 dB/mm (average). Given the tubular structure of the waveguides, such value can be considered reasonable. For single-mode PMMA waveguides, the reported loss was 0.42 dB/mm [31,32]. The measured absorption loss can be considered negligible (0.06 dB/mm).

To verify the optically induced birefringence properties of the PMMA/DR13 sample, we used the setup presented in Fig. 2(c), positioning the reading beam in a region of the sample with the absence of waveguides. Fig. 6 shows a typical graph of the transmittance as a function of the exposure time. Before turning on the writing beam (Ar^+ laser), since the polarizer and analyzer are crossed, no reading laser (HeNe) is observed on the camera. As the writing laser impinges the sample (point I), reading laser transmission increases due to the photoinduced birefringence. After turning off the writing beam (point II), the transmittance signal remains approximately constant (at about 40% of the value reached with the writing laser on), because of a residual birefringence caused by a permanent orientation of the azochromophores. Subsequently, we attempted to measure the optically induced birefringence in the fabricated waveguides. In this case, by using the setup described in Fig. 2(c) we coupled the reading beam in the waveguide. However, transmitted light was observed in the camera even before turning on the writing laser beam, indicating residual birefringence in the waveguide probably generated by stress during its fabrication. Such process prevented the measurement of the optically induced birefringence.

4. Conclusion

In summary, we successfully demonstrate the fabrication of waveguides in PMMA doped with Disperse Red 13 (DR13) by oscillator-only fs-laser micromachining. The produced waveguides

presents a tubular structure, exhibiting an annular intensity distribution of the coupled light. The averaged total loss of the produced waveguides is 0.8 dB/mm at 632.8 nm. Finally, we observed residual birefringence in the waveguides, probably related to stress generated during the fabrication, which hindered the determination of optically induced birefringence due to the presence of the azochromophore DR13.

Acknowledgements

Financial support from FAPESP (Fundação de Amparo à Pesquisa do Estado de São Paulo) (Process no 2011/12399-0 and Process no 2012/04794-9), CNPQ (Conselho Nacional de Desenvolvimento Científico e Tecnológico), CAPES (Coordenação de Aperfeiçoamento de Pessoal de Nível Superior) and the Air Force Office of Scientific Research (FA9550-12-1-0028) are acknowledged.

References

- [1] K. Minoshima, A.M. Kowalevicz, I. Hartl, E.P. Ippen, J.G. Fujimoto, *Opt. Lett.* 26 (2001) 1516.
- [2] A.M. Streltsov, N.F. Borrelli, *Opt. Lett.* 26 (2001) 42.
- [3] K. Yamada, W. Watanabe, T. Toma, K. Itoh, J. Nishii, *Opt. Lett.* 26 (2001) 19.
- [4] M. Will, S. Nolte, B.N. Chichkov, A. Tünnermann, *Appl. Opt.* 41 (2002) 4360.
- [5] W. Watanabe, T. Asano, K. Yamada, K. Itoh, J. Nishii, *Opt. Lett.* 28 (2003) 2491.
- [6] T. Shih, R.R. Gattass, C.R. Mendonca, E. Mazur, *Opt. Express* 15 (2007) 5809.
- [7] Y. Nasu, M. Kohtoku, Y. Hibino, *Opt. Lett.* 30 (2005) 723.
- [8] A.M. Kowalevicz, V. Sharma, E.P. Ippen, J.G. Fujimoto, K. Minoshima, *Opt. Lett.* 30 (2005) 1060.
- [9] L. Eldada, L.W. Shacklette, *IEEE J. Sel. Top. Quantum Electron.* 6 (2000) 54.
- [10] K.M. Davis, K. Miura, N. Sugimoto, K. Hirao, *Opt. Lett.* 21 (1996) 1729.
- [11] B.H. Cumpston, S.P. Ananthavel, S. Barlow, D.L. Dyer, J.E. Ehrlich, L.L. Erskine, A.A. Heikal, S.M. Kuebler, I.Y.S. Lee, D. McCord-Maughon, J.Q. Qin, H. Rockel, M. Rumi, X.L. Wu, S.R. Marder, J.W. Perry, *Nature* 398 (1999) 51.
- [12] S. Maruo, O. Nakamura, S. Kawata, *Opt. Lett.* 22 (1997) 132.
- [13] D.S. Correa, M.R. Cardoso, V. Tribuzi, L. Misoguti, C.R. Mendonca, *IEEE J. Sel. Top. Quantum Electron.* 18 (2012) 176.
- [14] J. Si, J. Qiu, J. Zhai, Y. Shen, K. Hirao, *Appl. Phys. Lett.* 80 (2002) 359.
- [15] A. Zoubir, C. Lopez, M. Richardson, K. Richardson, *Opt. Lett.* 29 (2004) 1840.
- [16] L.H. Slooff, A. van Blaaderen, A. Polman, G.A. Hebbink, S.I. Klink, F.C.J.M. Van Veggel, D.N. Reinhoudt, J.W. Hofstra, *J. Appl. Phys.* 91 (2002) 3955.
- [17] J.M.P. Almeida, V. Tribuzi, R.D. Fonseca, A.J.G. Otuka, P.H.D. Ferreira, V.R. Mastelaro, P. Brajato, A.C. Hernandez, A. Dev, T. Voss, D.S. Correa, C.R. Mendonca, *Opt. Mater.*
- [18] C.R. Mendonca, L.R. Cerami, T. Shih, R.W. Tilghman, T. Baldacchini, E. Mazur, *Opt. Express* 16 (2008) 200.
- [19] H. Zhang, D. Lu, M. Fallahi, *Opt. Mater.* 28 (2006) 992.
- [20] Y. Shi, C. Zhang, H. Zhang, J.H. Bechtel, L.R. Dalton, B.H. Robinson, W.H. Steier, *Science* 288 (2000) 119.
- [21] M. Jäger, G.I. Stegeman, S. Yilmaz, W. Wirges, W. Brinker, S. Bauer-Gogonea, S. Bauer, M. Ahlheim, M. Stähelin, B. Zysset, F. Lehr, M. Diemeer, M.C. Flipse, *J. Opt. Soc. Am. B: Opt. Phys.* 15 (1998) 781.
- [22] A. Natansohn, S. Xie, P. Rochon, *Macromolecules* 25 (1992) 5531.
- [23] P. Rochon, J. Gosselin, A. Natansohn, S. Xie, *Appl. Phys. Lett.* 60 (1992) 4.
- [24] J. Thomas, R. Bernard, K. Alt, A.K. Dharmadhikari, J.A. Dharmadhikari, A. Bhatnagar, C. Santhosh, D. Mathur, *Opt. Commun.* 304 (2013) 29.
- [25] J.W. Chan, T. Huser, S. Risbud, D.M. Krol, *Opt. Lett.* 26 (2001) 1726.
- [26] J.W. Chan, T.R. Huser, S.H. Risbud, J.S. Hayden, D.M. Krol, *Appl. Phys. Lett.* 82 (2003) 2371.
- [27] A. Zoubir, M. Richardson, C. Rivero, A. Schulte, C. Lopez, K. Richardson, N. Hô, R. Vallée, *Opt. Lett.* 29 (2004) 748.
- [28] S.M. Eaton, C. De Marco, R. Martinez-Vazquez, R. Ramponi, S. Turri, G. Cerullo, R. Osellame, *J. Biophotonics* 5 (2012) 687.
- [29] T. Gorelik, M. Will, S. Nolte, A. Tünnermann, U. Glatzel, *Appl. Phys. A* 76 (2003) 309.
- [30] J. Burghoff, C. Grebing, S. Nolte, A. Tünnermann, *Appl. Phys. Lett.* 89 (2006).
- [31] S. Sowa, W. Watanabe, T. Tamaki, J. Nishii, K. Itoh, *Opt. Express* 14 (2006) 291.
- [32] W. Watanabe, S. Sowa, T. Tamaki, K. Itoh, J. Nishii, *Jpn. J. Appl. Phys.*, 45 L765.